INTEGRAL-EQUATION METHOD FOR CALCULATION OF COUPLING IMPEDANCE FOR A VACUUM CHAMBER INHOMOGENEITY IN ACCELERATORS

S.S.Kurennoy and S.V.Purtov

Institute for High Energy Physics, Serpukhov, 142284, USSR

A method for calculation of coupling impedance produced by an inhomogeneity of vacuum chamber is developed. Both the inhomogeneity and vacuum chamber have to be of the same (axial or flat) type of symmetry. Boundary shape of inhomogeneity is given by a general single-valued function of the longitudinal coordinate. The method allows one to calculate impedances both at low frequencies and in resonance range. The interaction of a few insertions is also considered.

Introduction

Beam stability requirements are known to restrict the allowed values of the beam-chamber coupling impedances [1]. The impedances for a smooth chamber can be calculated easily [2], but the calculation of those produced by some chamber inhomogeneities, i.e., by bellows, junctions, etc, is a much more difficult problem.

Our paper develops a method allowing one to calculate the impedance for a single chamber element (group of elements), which is far enough from other inhomogeneities. In such a case it is convenient to study an idealized problem: let an inhomogeneity be placed on an infinite homogeneous beam pipe. The TBCI code [3] is usually used to compute the impedance for such a structure, but this way requires a lot of computer resources. There are also some other methods: paper [4] treats the case of particular inhomogeneity form (pillbox), and in Ref.[5] the impedance calculation is reduced to a numerical solution of a boundary problem by means of the SUPERFISH code [6]. Our method allows one to find semianalytically the coupling impedance for an inhomogeneity, which can be shaped quite generally, in a cylindrical chamber, as in Refs.[4,5], or in a flat one.

The method developed supplements the matrix one [7], (which calculates the impedance for an infinite periodic structure) being, actually, the analogy of the latter for nonperiodic structures.

1.Problem Formulation

A model of an accelerator vacuum chamber is considered: an infinite pipe having an inhomogeneity of length L. Let this system have an axial or flat geometry. The boundary shape is given by the function $r = b(z)$; $b(z) = b$ at $|z| \geqslant L/2$, where b is the smooth-chamber radius (half-height) (Fig.1). We assume that this function is single-valued, i.e. one and only one point $r = b(z)$ corresponds to any $z \in (-\infty,\infty)$.

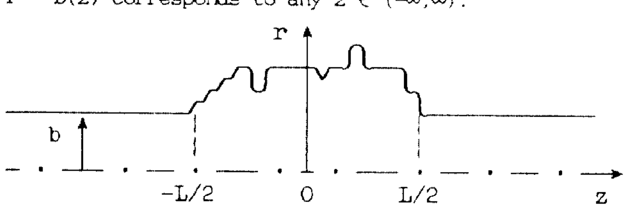

Fig.1. Layout of the problem.

Let the current perturbation wave travel along the chamber axis z:

$$j_z(z,r,t) = \rho(k_o)\beta c\, \exp(ik_o z - i\omega t)\ \theta(a-r), \quad (1)$$

where $\omega = \beta c k_o$, a is the beam radius. The solution to the Maxwell equations with current (1) is:

$$E_z(z,r) = \int_{-\infty}^{\infty} dk\, e^{ikz} \left[A(k) g(\chi_k r) + \delta(k-k_o) \begin{Bmatrix} -1 \\ p(\chi r) \end{Bmatrix} \right]; \quad (2)$$

and similarly for E_r and H_φ. In Eq.(2) $\chi_k^2 = k^2-(\omega/c)^2$; $\chi = \chi_{k_o} = k_o/\gamma$; the factor $i\rho(k_o)/\varepsilon_o k_o$ is dropped out; the upper line in {...} corresponds to $0<r<a$, the lower one to $r>a$ and the functions $g(x)$ and $p(x)$ are:

– in axisymmetric case

$$g(x) = I_o(x);\ p(x) = -\chi a (K_1(\chi a) I_o(x) + I_1(\chi a) K_o(x)); \quad (3a)$$

– for flat geometry

$$g(x) = \mathrm{ch}\, x\ ;\quad p(x) = -\mathrm{ch}(x-\chi a). \quad (3f)$$

The unknown function A(k) in Eqs.(2) is determined from the boundary conditions on the chamber wall:

$$\left[E_z + b'(z) E_r + (1-i)\frac{\delta\omega}{2c}\sqrt{1+(b'(z))^2}\, Z_o H_\varphi \right]_{r=b(z)} = 0. \quad (4)$$

Here $\delta = \sqrt{2/(\mu_o \sigma\omega)}$ is the skin-depth and σ is the conductivity of the wall material. Substituting field expressions (2) into Eq. (4), we get an integral equation for the function A(k). In particular, it is easily solved for a smooth pipe when $b(z) = b$:

$$A^{(o)}(k) = \delta(k-k_o) a^{(o)}(k_o) = = -\delta(k-k_o) \frac{p(\chi b) - (1+i)\eta p'(\chi b)/\chi b}{g(\chi b) - (1+i)\eta g'(\chi b)/\chi b}, \quad (5)$$

where p and g are defined in (3) and $\eta = \delta/2b\cdot(\omega b/c)^2$.

Substituting E_z (2) into the longitudinal impedance [2], we split A(k) into $A^{(o)}(k) + F(k)$, where $A^{(o)}(k)$ is defined by Eq.(5). As a result we get

$$Z(\omega) = -\frac{iZ_o}{\beta k_o S_\perp}(\bar{g} a^{(o)}(k_o) - 1)\int dz - \frac{2\pi i Z_o}{\beta k_o S_\perp}\bar{g} F(k_o). \quad (6)$$

The first term in RHS of Eq.(6), which is proportional to the vacuum-chamber length $L_{cham} = \int dz$, is just the smooth-pipe impedance and the second one is the impedance produced by the inhomogeneity itself. So, the inhomogeneity-produced impedance $Z(\omega)$ is related to $F(k_o)$.

2.The Integral Equation

1. Substituting Eqs.(2) into boundary condition (4) with account of $A(k) = \delta(k-k_o) a^{(o)}(k_o) + F(k)$, we obtain the following integral equation for F(k):

$$\int_{-\infty}^{\infty} dk\, e^{i(k-k_o)z} f[k,b(z),b'(z)] F(k) = q[b(z),b'(z)], \quad (7)$$

where

$$f[k,b(z),b'(z)] = g(\chi_k b(z)) - - g'(\chi b(z))/\chi b\cdot(ib'(z)kb + (1+i)\eta\sqrt{1+b'(z)^2});$$

$$q[b(z),b'(z)] = 1/(g-(1+i)\eta g'/x)\cdot \cdot\left\{ pg_z - p_z g + ib'(z)\frac{k_o b}{x}(p_z' g - p g_z') + (1+i)\frac{\eta}{x}\left[p_z g' - p' g_z + + ib'(z)\frac{k_o b}{x}(p_z' g' - p' g_z') + \sqrt{1+b'(z)^2}(p_z' g - p g_z') \right] \right\}.$$

In Eq.(7) the notations of Eq.(2) are used and $x=\chi b$, $p=p(\chi b)$, $g=g(\chi b)$, $p_z = p(\chi b(z))$, $g_z = g(\chi b(z))$.

The RHS of Eq.(7), $q[b(z),b'(z)]$, has the property that $q[b,0] = 0$. Hence, $q[b(z),b'(z)] = 0$ holds for each z satisfying $|z| \geqslant L/2$. It follows that for a smooth chamber, i.e., when $b(z) = b$, the solution to Eq.(7) is trivial, $F(k) = 0$. The RHS $q[b(z),b'(z)]$ can be easily expressed in an explicit form for a given symmetry.

Eq.(7), the Fredholm equation of the 1st kind, is an ill-posed problem [8] and, besides, is inconvenient for a numerical solution. Its Fourier transform, with account of $b(z) = b$ when $|z| > L/2$, yields the 2nd kind integral equation:

$$F(k) + \int_{-\infty}^{\infty} dk'\, K(k,k')\, F(k') = R(k)\ , \qquad (8)$$

in which

$$K(k,k') = \int_{-L/2}^{L/2} dz\, e^{-i(k-k')z}\, \frac{(f[k',b(z),b'(z)]-f[k',b,0])}{2\pi f[k,b,0]};$$

$$R(k) = \frac{1}{2\pi f[k,b,0]} \int_{-L/2}^{L/2} dz\, e^{-i(k-k_o)z}\, q[b(z),b'(z)]\ . \quad (9)$$

This equation is more convenient both for a numerical solution and for an analytical study. So, it is easy to construct the perturbation expansion over the powers of the kernel K for the solution of Eq.(8) by means of iterations. If $\varepsilon = \max(b(z)/b-1) \ll 1$, an ε-expansion can easily be obtained in analogy to what has been done for periodic structures [9].

2. The transition from a single perturbation (Fig.1) to N identical equidistant ones (Fig.2) is achieved by

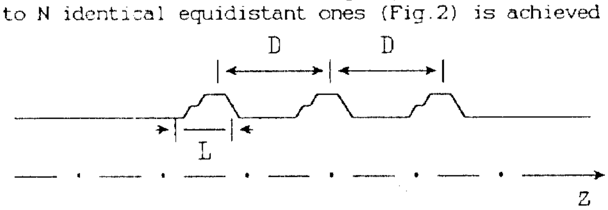

Fig.2. Group of identical equidistant inhomogeneities.

a simple modification of the kernel and RHS of Eq.(8):

$$K_N(k,k') = \Phi_N(k-k')\, K_1(k,k'),$$
$$R_N(k) = \Phi_N(k-k_o)\, R_1(k),$$

where

$$\Phi_N(x) = \begin{cases} \dfrac{\sin xND/2}{\sin xD/2}, & xD \neq 2\pi m \\ N, & xD = 2\pi m,\ m = 0, \pm 1 \dots \end{cases}$$

K_1 and R_1 are defined in Eq.(9). Note, that the matrix equation of Ref. [7] is obtained in the limit of $N \to \infty$.

3. Numerical Study of Integral Equation

1. In some cases the kernel K and RHS R of Eq.(8) can be expressed in an analytic form. But even in such a case a numerical solution of the integral equation seems inevitable. For this purpose it is necessary to cut the integration over k' up to a finite range, $[k_o-\Delta k, k_o+\Delta k]$. We choose cut-off $\Delta k = 2\pi\varkappa/\min(L,b)$, where $\varkappa$ is a dimensionless parameter. Then the integral equation is replaced by the following linear system:

$$F(k_i) + \sum_{j=1}^{M} w_j K(k_i,k_j) F(k_j) = R(k_i), \quad i=1,..M, \qquad (8')$$

where w_j, k_j are weights and points of M-point Gaussian quadrature on the $[k_o-\Delta k, k_o+\Delta k]$ interval. The independence of the results on the cut-off parameter $\varkappa$ and on the number of subdivision points, M, is a criterion for the results to be correct. Computations show that the program works well both in the low frequency range and for resonance calculations. But when frequencies are much above the chamber cut-off frequency, we must integrate fast-oscillating functions. The subdivision point number, M, has to be large in this case and the matrix in Eq.(8') becomes ill-defined. Hence, at these frequencies other, more refined, numerical procedures should be used to solve the integral equation.

The computation time has the M^2-dependence on the matrix size M and is also proportional to the subdision number N_{div} of the $[-L/2,L/2]$ interval when the kernel and RHS term are calculated numerically. Typical computation times (CPU ICL-1906A) for a single frequency are: for analytic kernel - 1-2s for $M \leqslant 32$; for numerical kernel - 15s at M = 15 and N_{div} = 16 in the flat chamber and twice that in the cylindrical one. It is seen that kernel computation takes most of this time.

2. <u>Low frequencies</u>. Calculations show that at frequencies, much lower than the chamber cut-off, Re $Z(\omega)$ is related only to an increase of the wall surface. When $\gamma \gg 1$ and $\sigma \to \infty$, Im $Z(\omega)$ is negative and proportional to frequency. So, both widenings and contractions of the chamber are inductive elements. If one denotes $h = \max\,(b(z)-b)$, then for $h \ll b$ the inductance behaves like $\mathrm{Im}Z \propto h^2$, and for $h \sim b$ usually as $\mathrm{Im}Z \propto h$. The dependence on the perturbation length at fixed h is as follows: $\mathrm{Im}Z(\omega)$ increases with L increase till $L \leqslant b$, and for large L it is almost L-independent.

Empirical formulae for the inductance $\mathcal{L} = \mathrm{Im}\, Z(\omega)/\omega$ of some typical discontinuities are obtained. For a chamber cavity, which has a triangular axial cross-section with base L and height h ($h \leqslant b$), we get:

$$\mathcal{L} = \frac{Z_o}{2\pi c}\cdot\frac{Lh}{B}\cdot\sin\theta = \frac{Z_o}{2\pi c}\cdot\frac{Lh}{B}\cdot 2h/\sqrt{L^2+4h^2}\ .$$

Here θ is the near-base angle, B is the width of a flat chamber and is replaced by πb in the case of a cylindrical chamber. For a chamber contraction having the same triangular cross-section, $\mathcal{L} = Z_o h^2/(2cB)$.

The inductance for a couple of transitions of length l from the chamber radius b to that of the insertion, b+h or b-h, for $l \ll L,b$ turns out to be almost independent of the distance L between transitions. When $L > b$, the inductance produced by a widening of the chamber is equal to that of a contraction with the same value of h. For $L \geqslant 2b$, the value of the inductance is approximated by $\mathcal{L} = Z_o h^2 \sqrt{\theta}\,/(2cB)$.

It should be noted that in paper [10] the low-frequency impedance for some simple discontinuities has been studied with the help of the TBCI code [3]. The results obtained and empirical formulae are similar to ours.

3. <u>Resonances</u>. As an example, we calculate resonances of the longitudinal impedance produced in the flat chamber with b = 3cm and $B = \pi b$ by a triangular-shaped cavity with the length L = 1cm along the beam direction. Figure 3 shows the results in the frequency range up to 14 GHz for the case when this insertion has the depth h = 0.5cm and the wall conductivity is $\sigma = 1.43/(\mu\Omega\cdot m)$. In these computations, M = 32 and $\varkappa = 2$ have been used. A typical resonance band-width is near 1 MHz. The resonance values of four lowest resonances vary with h-variation as shown in Fig.4. When h increases, resonance frequencies decrease monotonically but rather weakly, and they are quite near to the cut-off frequencies of different chamber modes, especially for small chamber perturbations.

Unlike time-domain methods for impedance calculations, which solve a nonstationary problem (the TBCI code being an example), our approach does not give a picture of the broad-band impedance for a single discontinuity at frequencies higher than the smooth chamber cut-off frequency. It is quite natural due to the problem formulation itself, because we consider a *stationary* picture in the frequency domain. Since an infinite structure is considered, the field energy is absorbed in the chamber walls, rather than leaks from the whole structure. This suggests that the real part of the impedance vanishes in the limit of perfectly conducting walls, i.e., Re $Z(\omega)$= 0 for any ω except for resonance frequencies. At the same time, it is known, that it is the energy leaking from the structure at $\omega > \omega_{cut}$ that leads to the broad-band impedance in time-domain calculations ($\mathrm{Re}Z(\omega) \neq 0$ for every $\omega > \omega_{cut}$).

Obviously, the nonstationary approach is adequate if fields induced by a particle bunch damp before the next bunch arrives, e.g. in LEP. The broad-band impedance picture is quite adequate in this case. In the opposite case (UNK, LHC, SSC) it is necessary to know a detailed impedance pattern and the stationary approach has to be used in calculations.

4. Group of inhomogeneities. Let us compare the impedance for a single insertion with that for a set of N equidistant insertions having the same form. This comparison can provide us with information on impedance additivity. Fig.5 shows Im Z/N at frequency 10 MHz versus N for a variable distance D between discontinuities. Here L = 1cm, h = 0.5cm and b = 3cm are taken. The value of Re Z/N is independent of N for any distance D. The picture shows that even at low frequencies the impedances of different elements are additive only when the distance between them is sufficiently large (D > 2b). So, the calculation of the low-frequency impedance for bellows from the impedance of a single corrugation, e.g. Ref.[11], yields only an approximate answer.

The resonant frequencies of the set of two identical elements with L = 1cm, h = 0.5cm and b = 3cm differ only slightly from those in the case of N = 1 (cf. Fig.3). However, the values of the resonances are strongly dependent on the distance D between elements. In Fig.6 the reduced values of impedance, Z_{res}/N, are compared with those in the case of N = 1 at different D's. The oscillations of Z_{res}/N are seen perfectly.

Conclusion

The integral-equation method for calculating the coupling impedance generalizes the matrix method [7] to nonperiodic structures. The above results show that the method can be successfully used to calculate the impedance for an arbitrary-shaped inhomogeneity both at low frequencies and in the resonance region.

This method can also be applied to calculate the transverse impedance in the same way as the matrix one [7]. Unlike the longitudinal case, after substituting fields into the boundary conditions we get a set of two coupled integral equations instead of integral equation (7) or (8). We do not present it here.

As in the numerical solution of Eq.(8) most of the CPU time is spent for computing the kernel, it seems to be promising to solve directly the 1st kind integral equation, Eq.(7), because its kernel is given in the explicit analytical form from the start.

More detail and discussion can be found in Ref.[12].

The authors would like to thank V.I.Balbekov for fruitful discussions and remarks.

References

1. A.Chao - Preprint SLAC-PUB-2946, Stanford, 1982.
2. E.Keil and B.Zotter -*Part.Acc.* v.3,p.11-20, 1972.
3. T.Weiland - ***NIM***, v.212, p.13-21, 1983.
4. H.Henke - Preprint CERN-LEP-RF/85-41, Geneva, 1985.
5. R.L.Gluckstern and F.Neri - In: Europ. Part. Accel. Conf., Rome, June 1988. - v.2, p.797-799.
6. K.Halbach, R.F.Holsinger -*Part.Acc*.v.7,p.213,1976
7. S.S.Kurennoy and S.V.Purtov - Preprint IHEP 89-1, Serpukhov, 1989.; *Part.Acc.*, v.24 (in press).
8. N.N.Kalitkin "Numerical Methods".-Msc: Nauka, 1978.
9. S.S.Kurennoy -Preprint IHEP 88-10, Serpukhov, 1988. S.S.Kurennoy and S.V.Purtov -In: Europ. Part Accel. Conf., Rome, June 1988. - v.1, p.761-763.
10. K.L.F.Bane - *ibid*, p.637-639.
11. K.-Y. Ng - Preprint FNAL FN-449, Batavia, 1987.
12. S.S.Kurennoy and S.V.Purtov - Preprint IHEP 90-31, Serpukhov, 1990.

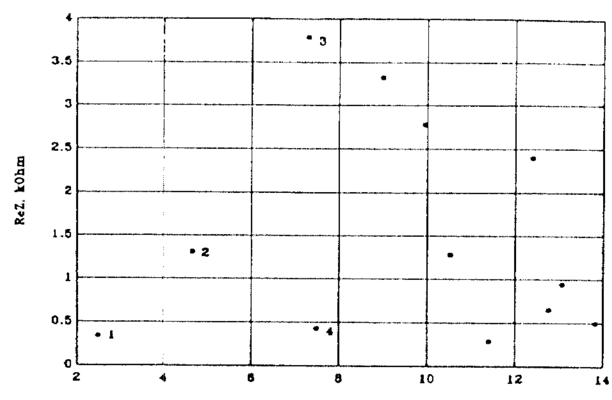

Fig.3 Resonances in frequency range up to 14 GHz (L = 1cm, h = 5 mm).

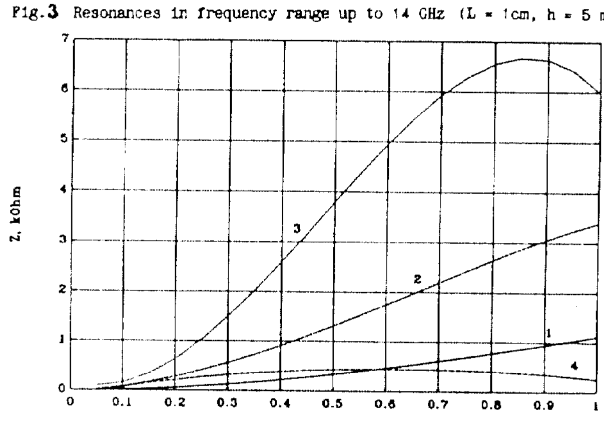

Fig.4 Values of resonances versus depth h of insertion for four lower resonances (see Fig.3).

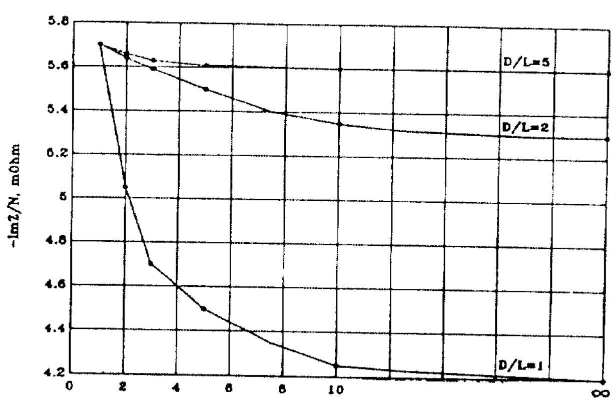

Fig.5 Imaginary part of impedance versus the number of inhomogeneities N for various distances between them. Values for N → ∞ are obtained by the matrix method [7].

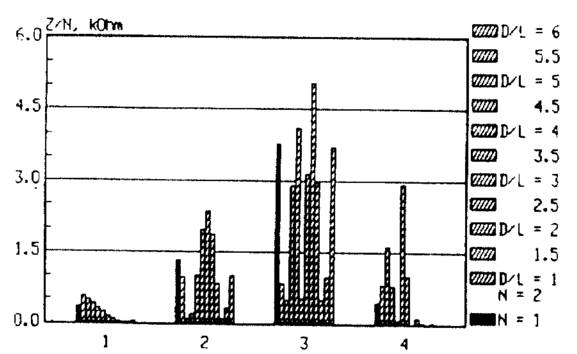

Fig.6 Values of resonances for various distances between insertions for four lower resonances. Dark columns: N = 1, and light ones: N = 2 for D/L = 1(0.5)6.